

Hexagonal array of impinging jets

L.F.G. Geers

1 Case description

1.1 Flow

Figures 1 and 2 show the flow configuration for the impinging jet array. Air from an open-circuit wind tunnel issued through a flat nozzle plate, after which it impinged on a horizontal glass plate. The end of the wind tunnel is a straight section with a square cross-section of $0.3 \times 0.3 \text{ m}^2$, providing a steady, low velocity air flow to the nozzle plate. The nozzle plate has a thickness of 2 mm and is provided with 13 nozzles with straight edges in a hexagonal arrangement. The diameter of the nozzles D_m is 13 mm, the nozzle spacing (pitch) s is 26 mm ($2D_m$). The distance between the nozzle plate and the impingement plate H was $4D_m$. The impingement section was open on all four sides providing free outflow of the spent air.

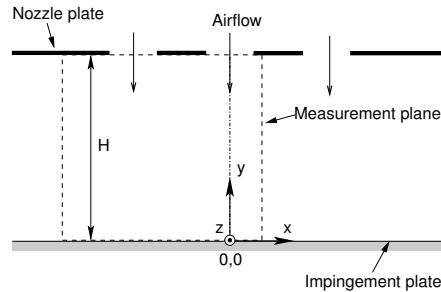


Figure 1: Flow configuration of hexagonal jet array for velocity and turbulence measurements.

The velocity and turbulence data presented in this case resulted from PIV measurements in two vertical planes parallel to the jet flow, as shown in Figures 1 and 2. Plane 1 intersects the central jet and one of its direct neighbors and plane 2 intersects the central jet and one of the outer jets. The origin of a x, y, z -coordinate system is at the intersection of the center line of the central jet and the surface of the impingement plate. The y -axis is measured along this centerline and assumed to be positive in the upward direction. The x - and z -axes are measured along the surface of the impingement plate. The position

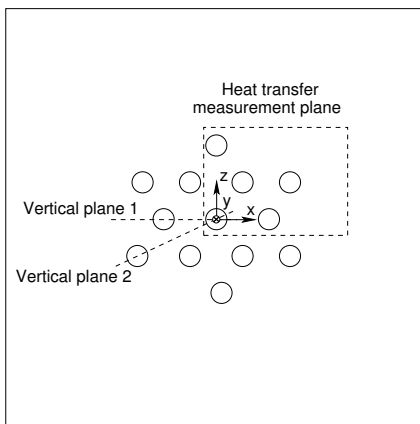


Figure 2: Orientation of the velocity and heat transfer measurement planes with respect to the nozzles.

of the measurement area for PIV in both planes was $-4.4 < x/D_m < 1.0$ and $0.0 < y/D_m < 4.0$.

1.2 Heat transfer

Heat transfer measurements were done on the impingement surface in the rectangular area depicted in Figure 2 with a size of about $6D_m \times 5D_m$. To this end the glass impingement plate used for the velocity measurements was replaced by a metal sheet of $25 \mu\text{m}$ thick. This sheet is stretched between two clamps, as can be seen in Figure 3. Two cylindrical supports bend the sheet downwards on both ends to prevent the clamps from disturbing the flow. The heat transfer measurements are done at the same conditions as the flow measurements (i.e. same nozzle plate, H , and Re).

The impingement sheet is heated electrically by means of a current source and the power dissipated in the sheet is measured using multimeters. The bottom side of the sheet is covered with a layer of black backing paint of about $5 \mu\text{m}$ and a layer of liquid crystals of about $15 \mu\text{m}$ thick to monitor the temperature of the sheet. The thickness of the liquid crystal layer proved to be sufficient for producing colors with sufficient saturation.

2 Measurements

2.1 Flow

The PIV system (manufactured by Optical Flow Systems, OFS) included a double pulsed Nd:YAG laser (Continuum Minilite) with a pulse energy of 25 mJ. This laser was used to produce a 1 mm thick sheet that illuminated the

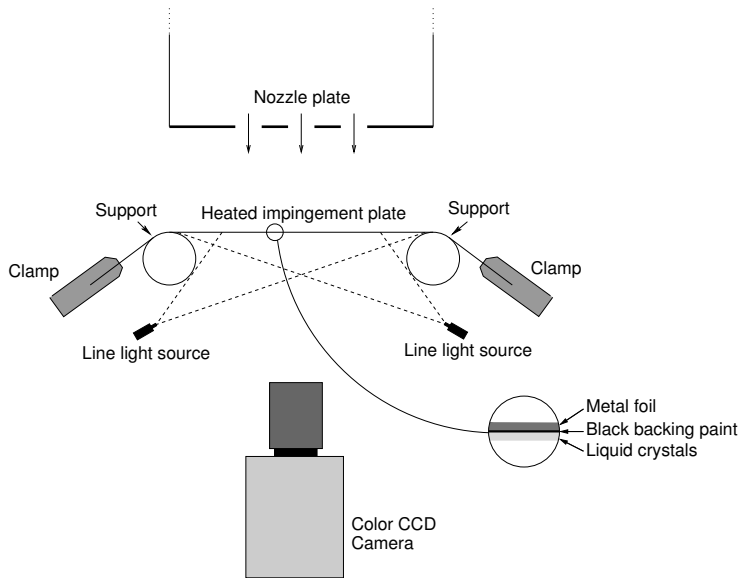


Figure 3: Experimental rig for temperature measurements on the impingement surface.

flow. A PCO SensiCam camera with a resolution of 1280×1024 pixels recorded images of the seeding particles in the laser sheet. The commercial software VidPIV Rowan v4.0 developed by OFS was used to analyze the images. Liquid droplets of about $1 \mu\text{m}$ in size were used as seeding.

For the recording camera a lens was used with a focal length of 105 mm and a numerical aperture of 11. The time delay between laser pulses was $20 \mu\text{s}$. The selected values for the time delays enabled measurements at a Reynolds number of 18.2×10^3 . In order to make reliable estimates of the mean velocity fields and the distributions of Reynolds stresses in the vertical planes, the ensembles in each plane counted 3000 image pairs.

The PIV images were analyzed in three consecutive steps. First, non-overlapping interrogation areas of 32×32 pixels were cross-correlated. A local median filter was used to discard the spurious vectors; the resulting empty spaces were filled with interpolated values from the surrounding interrogation areas. The resulting displacement fields were used as window displacements for an adaptive cross-correlation with non-overlapping interrogation areas of 32×32 pixels ($1.8 \times 1.8 \text{ mm}^2$) in the second step. With this configuration the dynamic velocity range of the PIV system is 0.3 to 22.5 m/s. After filtering out and replacing the spurious vectors with the same interpolation technique as was applied for the single jet data, the second step is repeated. The percentage of spurious vectors was 4% on average.

2.2 Heat transfer

Four 150 W light sources (DCR III, Schott-Fostec LLC) were used to illuminate the liquid crystals. The light from these sources is guided through four glass fiber bundles and transferred to two 13" Light Lines (Schott-Fostec, LLC). In these devices the fibers from the bundles are ordered to produce light lines of homogeneous intensity. The infra-red radiation that the crystals receive from the light source is reduced to a minimum by an IR-filter before the light is coupled into the fibers. The color temperature associated with the spectrum of the light is about 3200 K. A PCO SensiCam SVGA color camera was used to acquire snapshots of the liquid crystals. The camera contains a 2/3" CCD chip with 1280×1024 pixels that record the intensity of the incident light. The CCD chip is equipped with Bayer filters to distinguish colors.

The calibration of the liquid crystals is done in the same experimental rig as the measurements to keep lighting and viewing angles constant. Water of a known temperature is recirculated on the impingement plate to provide the crystals with a constant and known temperature at which their color is recorded. The temperature of the water is monitored using a Pt-100 probe. In this way, the temperature of the water was maintained within about 0.02 °C. The liquid crystals were calibrated at about 90 to 100 points spread over the full temperature range. Typically ten snapshots are taken from the liquid crystals at each (constant) temperature level. After that, all snapshots are processed by a local median test and a smoothing filter to remove salt-and-peper noise and color aliasing, and to diminish random noise. All snapshots at one temperature level are used to calculate average hue values and standard deviations of hue on each pixel position in the viewing area. Using the calibration curves local temperatures on the metal foil can be calculated.

The mean heat transfer was calculated from 200 images and the surface average uncertainty was about 2%.

3 Results

All data are presented in tab-separated ASCII files with a header stating some experimental conditions and the quantities presented in the table that follows. The flow results are presented in four files (horizontal and vertical profiles for both planes), the heat transfer data in only one file.

3.1 Flow

All velocity values are non-dimensionalized by the center line exit velocity of the center jet, U_{CL} , all Reynolds stresses and k by U_{CL}^2 , the wall-normal and wall-parallel distances by the nozzle diameter D_m , and the normal and shear components of P_k (i.e. production of kinetic energy) with U_{CL}^3/D_m . The turbulent kinetic energy k was estimated from the two-component PIV data as $1/2 \cdot (2\langle u'^2 \rangle + \langle v'^2 \rangle)$, assuming that the magnitude of the unmeasured (out-of-plane) third velocity component $\langle w'^2 \rangle$ was comparable to that of $\langle u'^2 \rangle$. The

normal component of P_k was estimated by

$$P_{uu} + P_{vv} = -\langle u'^2 \rangle \frac{\partial \langle u \rangle}{\partial x} - \langle v'^2 \rangle \frac{\partial \langle v \rangle}{\partial y} \quad (1)$$

and the shear component was estimated by

$$P_{uv} = -\langle u'v' \rangle \left(\frac{\partial \langle u \rangle}{\partial y} + \frac{\partial \langle v \rangle}{\partial x} \right) \quad . \quad (2)$$

Horizontal profiles are presented at $y = 0.25D_m, 0.5D_m, 1.0D_m, 1.5D_m, 2.5D_m,$ and $3.5D_m$ for vertical planes 1 and 2. The resolution in the area $y/D_m > 1.5$ seems insufficient for resolving thin shear layers at the jets edges (hence peaks in the curves), but this does not affect the general quality of the results, especially since we were interested more in the impingement area. Vertical profiles are presented at $x = -3.0D_m, -2.0D_m, -1.5D_m, -1.25D_m, -1.0D_m, -0.75D_m, -0.5D_m,$ and $0.0D_m$ for vertical plane 1 and at $x = -4.0D_m, -2\sqrt{3}D_m$ (i.e. centre of outer nozzle), $(-2\sqrt{3} + 0.5)D_m,$ $(-2\sqrt{3} + 0.75)D_m,$ $-\sqrt{3}D_m, -0.75D_m, -0.5D_m,$ and $0.0D_m$ for vertical plane 2.

A more detailed treatise of the velocity and turbulence measurements in this case can be found in Geers et al. (2004) and Geers (2003).

3.2 Heat transfer

The heat transfer data presented in this case were taken at the intersecting lines of the impingement plane and either of the above mentioned velocity measurement planes. The coordinates of sample points on these lines may not coincide with the sample coordinates of the velocity measurement planes, because the cameras used for both measurement techniques do not have equal resolution and alignment.

Profiles of the mean Nusselt number $\langle Nu \rangle = h_j D_m / \lambda_{air}$ are presented, in which h_j is the measured heat transfer coefficient due to the impinging jets and λ_{air} is the heat conductivity of the impinging air. Again the wall-parallel distance to the center jet is non-dimensionalized by D_m .

A more detailed treatise of the heat transfer measurements in this case can be found in Geers (2003).

References

- L. F. G. Geers. *Multiple impinging jet arrays: An experimental study on flow and heat transfer*. PhD thesis, Delft University of Technology, 2003.
- L. F. G. Geers, M. J. Tummers, and K. Hanjalić. Experimental investigation of impinging jet arrays. *Exp. Fluids*, 36:946–958, 2004.